

# Trapping an isotopic mixture of fermionic $^{84}\text{Rb}$ and bosonic $^{87}\text{Rb}$ atoms

S. G. Crane,<sup>1,2</sup> X. Zhao,<sup>1</sup> W. Taylor,<sup>1</sup> and D. J. Vieira<sup>1</sup>

<sup>1</sup>*Los Alamos National Laboratory, Los Alamos, New Mexico 87545*

<sup>2</sup>*Department of Physics, Utah State University, Logan, Utah 84322*

(Received 3 January 2000; published 13 June 2000)

We have simultaneously confined fermionic  $^{84}\text{Rb}$  and bosonic  $^{87}\text{Rb}$  atoms in overlapping magneto-optical traps in which radioactive  $^{84}\text{Rb}$  atoms ( $t_{1/2}=33$  d) have been trapped. We investigated  $^{84}\text{Rb}$  trap loss when overlapped with a cloud of  $^{87}\text{Rb}$  atoms trapped from a background rubidium vapor. Collision loss measurements were taken with  $\sim 5 \times 10^5$  and  $\sim 4 \times 10^7$  atoms of trapped  $^{84}\text{Rb}$  and  $^{87}\text{Rb}$ , respectively. We have found a trapping solution for which there is negligible additional trap loss for  $^{84}\text{Rb}$  due to the presence of  $^{87}\text{Rb}$ , showing that the mixture can be readily prepared for a sympathetic cooling experiment.

PACS number(s): 32.80.Pj, 05.30.Fk, 34.50.Rk, 29.25.Rm

The creation of very cold atomic vapor systems is an exciting new arena in which one can study macroscopic effects of quantum mechanics. A great deal of success has been achieved in cooling large numbers of bosonic atoms, which have been shown to collapse into a single motional ground state, known as a Bose-Einstein condensate (BEC) [1]. This work has spawned interest in cooling dilute Fermi systems to a quantum degenerate regime as well. Interesting properties such as linewidth narrowing and the suppression of inelastic collisions have been predicted [2] at phase-space densities comparable to those achieved in BEC experiments. A BCS-type phase transition to a superfluid state may also be observed at still lower temperatures depending on the coupling strength between the cold atoms [3].

For fermionic atoms in identical spin states,  $s$ -wave collisions are forbidden and  $p$ -wave collisions vanish at low temperatures, which brings evaporative cooling to a halt [4]. One method of avoiding this limitation, sympathetic cooling using two different spin states, has already shown promising results in  $^{40}\text{K}$  [5]. However, there are only two naturally occurring fermionic alkali-metal atoms,  $^6\text{Li}$  and  $^{40}\text{K}$ , which severely limits the number of systems that can be studied. An intriguing alternative is the possibility of trapping radioactive fermionic atoms and cooling them sympathetically with a system of cold, stable bosonic atoms. Recent calculations [6] show that  $^{84}\text{Rb}$  ( $t_{1/2}=33$  d) is a good fermionic candidate because of its large and positive scattering length with  $^{87}\text{Rb}$  ( $a_s=117$  a.u. and  $a_T=550$  a.u.), which should allow for efficient sympathetic cooling [7]. A relatively low-field ( $B \approx 100$  G) Feshbach resonance is also predicted for the  $^{84}\text{Rb}$  ( $5S_{1/2}$ ,  $F=5/2$ ,  $m_F=5/2$ ) and ( $5S_{1/2}$ ,  $F=5/2$ ,  $m_F=3/2$ ) states [6]. This may provide a means to control the interaction between cold  $^{84}\text{Rb}$  atoms, effectively tuning the BCS phase transition temperature. Thus  $^{84}\text{Rb}$  and  $^{87}\text{Rb}$  offer an interesting system where a mixture of fermionic and bosonic quantum degeneracy may be realized. In this paper, we report on the loading of a magneto-optical trap (MOT) with radioactive  $^{84}\text{Rb}$  atoms and on the simultaneous trapping of  $^{84}\text{Rb}$  and  $^{87}\text{Rb}$  as an initial step toward a sympathetic cooling experiment. Trap loss of  $^{84}\text{Rb}$  is also investigated with and without an overlapped cloud of  $^{87}\text{Rb}$ .

The method used to trap radioactive  $^{84}\text{Rb}$  atoms is similar to that reported earlier for  $^{82}\text{Rb}$  [8].  $^{84}\text{Rb}$  atoms are produced

in 750-MeV proton spallation reactions on a molybdenum target at the Los Alamos Neutron Scattering Center. After irradiation, the target is transferred to a hot-cell facility where it is dissolved in hydrogen peroxide and the rubidium fraction is chemically extracted and precipitated as  $\text{Rb}_2\text{CO}_3$ . A radioactive sample containing 650  $\mu\text{Ci}$  of  $^{84}\text{Rb}$  was loaded into a tantalum crucible and installed in the ion source of a mass separator. The radioactive sample also contained 8 mCi of  $^{83}\text{Rb}$  ( $t_{1/2}=86$  d) which was also trapped but not discussed further here [9]. We monitor the amount of  $^{84}\text{Rb}$  activity in the ion source using a collimated NaI counter to detect the number of 886 keV  $\gamma$  rays associated with electron capture of  $^{84}\text{Rb}$ . The ion source was run at a setting that provided a moderate vaporization rate while maintaining a reasonably high degree of ionization for rubidium by controlling the temperature (typically  $\sim 950^\circ\text{C}$ ) at the tip of the crucible via electron bombardment heating. In this way, an ion beam was obtained with an intensity of  $\sim 2 \times 10^8$   $^{84}\text{Rb}^+$  ions/s that lasted for several weeks. The extracted beam is mass separated, collimated, and focused through a 5-mm  $\phi$  opening into a dry-film-coated, trapping cell (a 7.6-cm quartz cube), and implanted into an yttrium catcher foil located at the far corner of the cell. After a suitable accumulation period (10–120 min), the catcher foil is inductively heated ( $\sim 750^\circ\text{C}$ ) to release the implanted activity into the quartz cell as an atomic vapor where the  $^{84}\text{Rb}$  atoms are trapped. Due to the slow decay rate of  $^{84}\text{Rb}$ , it was not possible to determine a release efficiency from the catcher foil by using  $\gamma$  counting; however, based on our earlier measurements with  $^{82}\text{Rb}$  [8] we assume that our release efficiency is on the order of 20%.

The atomic energy levels relevant to the trapping of  $^{84}\text{Rb}$  [10] are shown in Fig. 1(a). The  $^{84}\text{Rb}$  magneto-optical trap (MOT) uses large-diameter (50 mm  $\phi$ , 100 mm  $1/e^2$  width), high-intensity (8 mW/cm<sup>2</sup> per beam) laser beams to increase the trapping efficiency. Three beams are derived from a Coherent 899-21 ring laser and used in the standard retro-reflected configuration with an axial field gradient of 7 G/cm to form the MOT. We use a feature in the  $^{85}\text{Rb}$  frequency modulated saturated absorption spectrum between the  $5S_{1/2}$ ,  $F=2 \rightarrow 5P_{3/2}$ ,  $F'=1$  and  $F'=1,2$  crossover peaks [see Fig. 1(b)] that is measured to be 89 MHz to the red of the  $^{85}\text{Rb}$

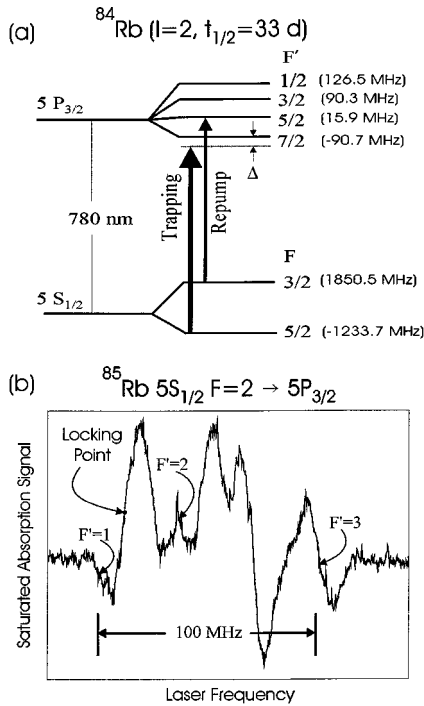


FIG. 1. (a) The  $^{84}\text{Rb}$  atomic energy levels (not shown to scale) relevant for atomic trapping are taken from Ref. [10]. The trapping and repump transitions are shown, where the trapping transition is detuned by the quantity  $\Delta$ . (b) The Rb reference cell frequency-modulated saturated absorption signal of the  $^{85}\text{Rb}$   $F=2 \rightarrow F'=1,2,3$  transitions. The locking point (shown as a solid circle) is used as a reference for the  $^{84}\text{Rb}$  trapping laser. The locking point is measured to be 89 MHz to the red of the  $^{85}\text{Rb}$   $F=2 \rightarrow F'=3$  transition.

$5S_{1/2}$ ,  $F=2 \rightarrow 5P_{3/2}$ ,  $F'=3$  transition as the locking reference point for the  $^{84}\text{Rb}$  trapping beam. We shift the frequency of the trapping beam from this locking point using a combination of acousto-optic modulators (AOMs) on the laser reference arm to give an overall shift of  $\nu_{\text{trap}}^{84} - \nu_{\text{locking point}}^{85} = -557$  MHz. This gives a detuning from the  $5S_{1/2}$ ,  $F=5/2 \rightarrow 5P_{3/2}$ ,  $F'=3/2$  cycling transition of  $\Delta \approx -15$  MHz. An electro-optic modulator (EOM) is placed in the main beam and driven at 1.480 GHz so that its second lower sideband will generate the repumping transition in  $^{84}\text{Rb}$  ( $\nu_{\text{repump}}^{84} - \nu_{\text{trap}}^{84} = -2.960$  GHz). The system has the beneficial feature of being able to trap  $^{85}\text{Rb}$  (introduced via a getter source) by locking the laser 15 MHz to the red of the  $^{85}\text{Rb}$  trapping transition and adjusting the repump EOM drive frequency to 1.464 GHz. This allows optimization of the  $^{84}\text{Rb}$  MOT setup (referred to hereafter as MOT I) with  $^{85}\text{Rb}$  before we begin experiments with radioactive species.

The trapping light for the  $^{87}\text{Rb}$  MOT setup (referred to as MOT II) is generated from a second Coherent 899-21 ring laser locked with a detuning of  $\Delta \approx -8$  MHz from the  $^{87}\text{Rb}$   $5S_{1/2}$ ,  $F=2 \rightarrow 5P_{3/2}$ ,  $F'=3$  trapping transition. MOT II has a combined six-beam intensity of 12 mW/cm<sup>2</sup>. A second EOM driven at 6.834 GHz provides the  $^{87}\text{Rb}$  repump. The  $^{87}\text{Rb}$  laser beam is brought in collinear with the  $^{84}\text{Rb}$  trapping beam just before the expansion and beam-splitting op-

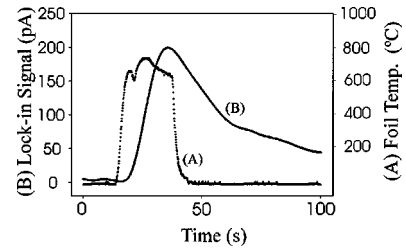


FIG. 2. A typical trapping signal showing the time sequence for the pulsed released and trapping of  $^{84}\text{Rb}$  that has accumulated in the yttrium catcher foil for two hours. Trace (A) is the foil temperature as measured with an optical pyrometer. Trace (B) shows the lock-in trapping fluorescence signal for  $^{84}\text{Rb}$  as measured with a calibrated photodiode. The lock-in amplifier has an integration time constant of 3 s.

tics that lead to the trapping cell. The fluorescence from the trapped cloud of  $^{84}\text{Rb}$  ( $^{87}\text{Rb}$ ) is modulated at 4.2 (6.0) kHz by switching the repump EOMs on and off at their respective frequencies. The fluorescent light is then focused through a 100- $\mu\text{m}$  pinhole onto a photomultiplier tube (PMT) or a calibrated photodiode using a 58-mm  $f/1.4$  lens and demodulated using lock-in amplifiers in order to reject background due to laser light scattering from the trapping cell surfaces. To ensure good spatial overlap of the  $^{84}\text{Rb}$  and  $^{87}\text{Rb}$  trapped clouds, we view the trapping region with two charged-coupled device (CCD) cameras positioned at different angles. Using nearly equivalent sized clouds ( $\sim 1$  mm $\phi$ ) of  $^{85}\text{Rb}$  in MOT I and  $^{87}\text{Rb}$  in MOT II, we adjust the laser alignment until both cameras show minimal spatial deviation when one or the other MOT laser beam is blocked.  $^{85}\text{Rb}$  trapped in MOT I was used for this overlapping procedure because the  $^{84}\text{Rb}$  clouds were not typically visible on the CCDs. The  $^{84}\text{Rb}$  cloud in MOT I and  $^{85}\text{Rb}$  in MOT I were shown to occupy the same space in the trapping cell by doing careful position scans using the PMT.

A typical trapping signal for  $^{84}\text{Rb}$  is shown in Fig. 2. These data were taken after  $^{84}\text{Rb}$  ions had been implanted in the foil for two hours. As the foil temperature rises (trace A)  $^{84}\text{Rb}$  is released into the cell and becomes trapped as indicated by the lock-in trapping signal (trace B). We used a calibrated photodiode with a 1-mm  $\phi$  pinhole to determine the number of trapped atoms. In a calibration run, we implanted  $^{84}\text{Rb}$  at a rate of  $2 \times 10^8$  ions/s for 30 minutes. Upon releasing, we observed a trapping signal corresponding to  $\sim 1.5 \times 10^5$  atoms. This gives a trapping efficiency of  $\sim 2 \times 10^{-6}$ , which is  $\sim 250$  times lower than the efficiency we achieved in trapping  $^{82}\text{Rb}$  [8]. We attribute this drop in trapping efficiency to the degradation of the dryfilm coating. This is supported by comparison to a trapping efficiency estimate for single-pass-trapping of hot atoms emitted directly from the foil (i.e., without ‘‘bouncing’’ or temperature re-equilibration with the cell walls). Subsequent cell coatings using SC-77 type dryfilm have yielded trapping efficiencies of  $\sim 10^{-2}$  in  $^{82}\text{Rb}$ . The cause of the dryfilm coating degradation was found to be the continuous heating of the yttrium foil for several hours at temperatures of  $\sim 750^\circ\text{C}$ . We have corrected for this problem by switching to a zirconium foil, which releases  $\sim 60\%$  of implanted  $^{82}\text{Rb}$  at  $\sim 750^\circ\text{C}$  and

has a significantly lower vapor pressure than yttrium at the same temperature. We also run in a pulsed-heating mode to limit the amount of time that the foil remains at high temperatures (release from the hot foil occurs in less than 3 s).

In order to perform the steps required for loading a fermionic and bosonic mixture into a magnetic trap designed for the sympathetic cooling experiment, it is helpful to obtain long mixed isotope ( $^{84}\text{Rb} + ^{87}\text{Rb}$ ) MOT lifetimes. To this end, we investigated  $^{84}\text{Rb}$  lifetimes with and without an overlapped cloud of  $^{87}\text{Rb}$ . The release of Rb atoms is quickly stopped when the foil heating is turned off (it takes  $\sim 1$  s for the foil to return to room temperature). The decay of  $^{84}\text{Rb}$  atoms from a MOT can therefore be described by

$$\frac{dN_{84}}{dt} = -\gamma N_{84} - \beta_{84,84} \int_{V_{84}} n_{84}^2 dV, \quad (1)$$

where  $N_{84}$  is the number of  $^{84}\text{Rb}$  in the MOT,  $V_{84}$  is the volume of the  $^{84}\text{Rb}$  cloud,  $\gamma$  is the loss rate for collisions with hot background gas,  $\beta_{84,84}$  is the loss rate for light-assisted collisions between trapped  $^{84}\text{Rb}$  atoms, and  $n_{84}$  is the  $^{84}\text{Rb}$  trapped cloud density. We can avoid an analytical solution of Eq. (2) by looking at two trapping regimes. The first is the constant density regime that occurs when there is a large number of atoms in the trap, in our case  $\geq 10^5$ . In this regime, the density ( $n_{84}$ ) of the MOT remains constant and the size of the cloud shrinks as the trap depletes [11]. In this case, the right-hand side (rhs) of Eq. (2) can be simplified to  $-(\gamma + \beta_{84,84} n_{84}) N_{84}$ , and we therefore have a pure exponential decay with rate constant  $1/\tau_1 = (\gamma + \beta_{84,84} n_{84})$ . After the number of atoms is reduced to  $< 10^4$ , the MOT moves into a different regime where the volume remains approximately constant, but the density diminishes. Since the light-assisted collision term scales as  $n_{84}^2$ , the trap loss will eventually be dominated by background gas collisions as the density decreases, leaving  $-\gamma N_{84}$  on the rhs of Eq. (2), which also results in a single exponential decay ( $1/\tau_2 = \gamma$ ).

By measuring the fluorescence decay from the  $^{84}\text{Rb}$  MOT, we find that the lifetime fits very well a double exponential decay (see Fig. 3) when more than  $10^5$  atoms are initially loaded into the trap. The difference in lifetime for the short-lived [ $\tau_1 = 12.8$  (0.7) s] as compared to the long-lived component [ $\tau_2 = 59$  (3) s] of the trap fluorescence decay curve indicates that light-assisted collisions are the dominant mechanism for trap loss in the constant density regime (at early times) and decrease in significance as the trap depletes, until the lifetime is limited only by background gas collisions. The measurement was taken with a total six-beam laser intensity of  $48 \text{ mW/cm}^2$ ,  $^{84}\text{Rb}$  trapping transition detuning of  $\Delta \approx -15 \text{ MHz}$ , and a constant  $^{84}\text{Rb}$  density of  $3 \times 10^{10} \text{ cm}^{-3}$  based on cloud fluorescence and size measurements. Using the constant density approximation for Eq. (2) at early times, we obtain a light-assisted collision trap loss rate of  $\beta_{84,84} = 3(1) \times 10^{-12} \text{ cm}^3 \text{ s}^{-1}$ , which is in the same range as previous homonuclear light-assisted collision loss rates measured for  $^{85}\text{Rb}$  and  $^{87}\text{Rb}$  under similar trapping conditions [12]. The uncertainty for  $\beta_{84,84}$  is mainly due to the absolute uncertainty in measured trapped cloud density that is estimated to be 30%.

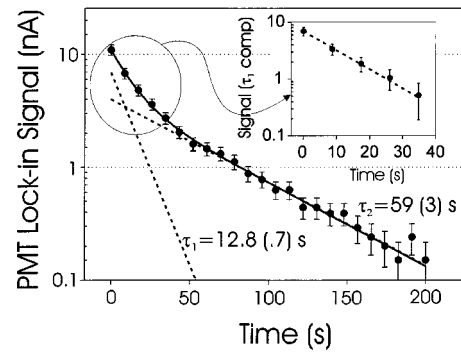


FIG. 3. Plot showing the decay of half a million  $^{84}\text{Rb}$  atoms from a MOT. The data fit well to a double exponential decay (solid line), indicating that there are two loss mechanisms that dominate for different MOT regimes. At early times, light-assisted collisions between trapped  $^{84}\text{Rb}$  atoms dominate the trap lifetime giving rise to the short-lived component ( $\tau_1$ ). As the density of the trap is reduced, light-assisted collisions become less important and collisions with the hot background gas become the main loss mechanism that yields the long-lived decay component ( $\tau_2$ ). The dashed lines are a visual aid showing the long and short-lived components separately, whereas the solid line is a fit to the experimental data. The inset on the upper right corner is a difference plot for the early part of the decay that clearly shows a good fit to the fast-lived component.

We then determined the mixed isotope loss rate for a trapped cloud of  $^{84}\text{Rb}$  overlapped with a cloud of  $^{87}\text{Rb}$ . To do this, we prepared a stable  $^{87}\text{Rb}$  cloud trapped from a vapor as introduced via rubidium getter and then overlapped this with a trapped cloud of  $^{84}\text{Rb}$  atoms as released from the catcher foil. The  $^{84}\text{Rb}$  decay curve is now governed by the following

$$\frac{dN_{84}}{dt} = -\gamma N_{84} - \beta_{84,84} \int_{V_{84}} n_{84}^2 dV - \beta_{87,84} \int_{V_{84}} n_{87} n_{84} dV, \quad (2)$$

where the additional term arises from the mixed isotope light-assisted collision loss rate  $\beta_{87,84}$ . By measuring the short-lived component ( $\tau_1$ ) of the  $^{84}\text{Rb}$  signal with and without the  $^{87}\text{Rb}$  cloud present, we could determine if any additional loss was introduced due to mixed isotope collisions. Measurements were taken when both species were in the constant density regime with  $\sim 5 \times 10^5$  trapped  $^{84}\text{Rb}$  atoms in MOT I and  $\sim 4 \times 10^7$   $^{87}\text{Rb}$  atoms in MOT II (see Fig. 4). Fitting the  $^{84}\text{Rb}$  lifetime in this regime gives  $\tau_1 = 13.4$  (0.7) s without the  $^{87}\text{Rb}$  cloud and  $\tau_1 = 11.1$  (0.5) s with the  $^{87}\text{Rb}$  cloud overlapped. The  $^{87}\text{Rb}$  and  $^{84}\text{Rb}$  MOT densities were both measured to be  $3 \times 10^{10} \text{ cm}^{-3}$ , which when combined with the difference in lifetime gives a  $\beta_{87,84} = 5(3) \times 10^{-13} \text{ cm}^3 \text{ s}^{-1}$ . This value was measured with a six beam laser intensity for  $^{87}\text{Rb}$  ( $^{84}\text{Rb}$ ) in MOT II (I) of  $12 \text{ mW/cm}^2$  ( $48 \text{ mW/cm}^2$ ) and trapping transition detuning of  $\Delta_{87} \approx -8 \text{ MHz}$  ( $\Delta_{84} \approx -15 \text{ MHz}$ ). Under these conditions,  $\beta_{87,84}$  is small because the low trapping light intensity used for  $^{87}\text{Rb}$  in MOT II reduces the likelihood for light-assisted collisions that involve excited  $^{87}\text{Rb}$  atoms. This is supported by a  $\sim 60$

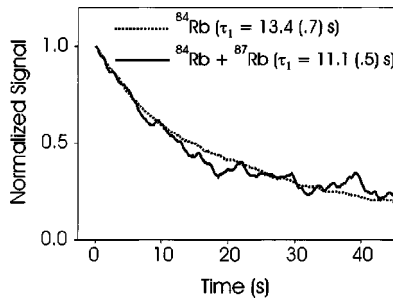


FIG. 4. Normalized trap lifetime measurements for  $^{84}\text{Rb}$  without (dotted line) and with (solid gray line) an overlapped cloud of  $^{87}\text{Rb}$ . These data were taken with both  $^{84}\text{Rb}$  in MOT I and  $^{87}\text{Rb}$  in MOT II under the constant density regime. Numerical fits of the data yield the short-lived lifetime ( $\tau_1$ ) for each case.

s fill-time measurement for  $^{87}\text{Rb}$  alone, which indicates that the lifetime is limited only by hot background gas collisions and that light-assisted collisions for  $^{87}\text{Rb}$  in MOT II are inconsequential. This shows that under these trapping conditions a  $^{84}\text{Rb}$  and  $^{87}\text{Rb}$  mixture can be simultaneously trapped in overlapping MOTs without significant additional loss of  $^{84}\text{Rb}$ . Moreover, without a significant change in MOT lifetime, the loading of the magnetic trap for the sympathetic cooling experiment is not very time critical.

Our future plans for the sympathetic cooling experiment are to complete construction of the magnetic trap and to couple it to the first trapping cell. A trapped mixture of  $^{84}\text{Rb}$

and  $^{87}\text{Rb}$  will then be transferred to the second cell from which they will be loaded into a time-orbiting potential (TOP) trap [13]. We have already gained considerable experience in MOT to MOT transfer and the loading of atoms into a TOP trap during an  $^{82}\text{Rb}$   $\beta$ -asymmetry experiment [14].

In summary, we have trapped radioactive  $^{84}\text{Rb}$  atoms and demonstrated the simultaneous trapping of a  $^{84}\text{Rb}$  and  $^{87}\text{Rb}$  mixture in overlapping magneto-optical traps. We have also found trapping parameters for which the addition of a stable  $^{87}\text{Rb}$  cloud does not significantly affect the trap lifetime of the  $^{84}\text{Rb}$  MOT. With cell coating improvements, it now appears promising to trap a sufficient number of  $^{84}\text{Rb}$  atoms to proceed with the sympathetic cooling of  $^{84}\text{Rb}$  with a Bose-Einstein condensate of  $^{87}\text{Rb}$  in order to produce and study Fermi degeneracy in  $^{84}\text{Rb}$  as well as to explore mixtures of ultracold fermionic and bosonic matter.

We thank Frank Albeelen, James Burke, Eric Cornell, Steve Lamoreaux, and Boudierjwn Verhaar for many helpful discussions related to this project. We also thank L. D. Benham, M. Archer, and the Chemistry Science and Technology Division machine shop for their excellent technical support. Special thanks also goes to Eric Burt of the U.S. Naval Observatory for work that will be instrumental in the next stage of this experiment. This work was supported in large part by the Laboratory Directed Research and Development program at Los Alamos National Laboratory, operated by the University of California for the U. S. Department of Energy.

- 
- [1] M.H. Anderson, J.R. Ensher, M.R. Mathews, C.E. Wieman, and E.A. Cornell, *Science* **269**, 198 (1995); K.B. Davis, M.O. Mewes, M.R. Andrews, N.J. van Druten, D.S. Durfee, D.M. Kurn, and W. Ketterle, *Phys. Rev. Lett.* **75**, 3969 (1995); C.C. Bradley, C.A. Sackett, J.J. Tollett, and R.G. Hulet, *ibid.* **75**, 1687 (1995); **79**, 1170 (1997).
  - [2] J.M.V.A. Koelman, H.T.C. Stoof, B.J. Verhaar, and J.T.M. Walraven, *Phys. Rev. Lett.* **59**, 676 (1987); A. Imamoglu and L. You, *Phys. Rev. A* **50**, 2642 (1994); J. Javanainen and J. Ruostekoski, *ibid.* **52**, 3033 (1995); T. Busch, J.R. Anglin, J.I. Cirac, and P. Zoller, *Europhys. Lett.* **44**, 1 (1998).
  - [3] M. Houbier, R. Ferwerda, H.T.C. Stoof, W.I. McAlexander, C.A. Sackett, and R.G. Hulet, *Phys. Rev. A* **56**, 4864 (1997).
  - [4] H.F. Hess, *Phys. Rev. B* **34**, 3476 (1986); H.F. Hess, G.P. Kochanski, J.M. Doyle, N. Masuhara, D. Kleppner, and T.J. Greytak, *Phys. Rev. Lett.* **59**, 672 (1987).
  - [5] B. DeMarco and D.S. Jin, *Science* **285**, 1703 (1999).
  - [6] J.P. Burke, Jr. and J.L. Bohn, *Phys. Rev. A* **59**, 1303 (1999).
  - [7] C.J. Myatt, E.A. Burt, R.W. Ghrist, E.A. Cornell, and C.E. Wieman, *Phys. Rev. Lett.* **78**, 586 (1997).
  - [8] R. Guckert, X. Zhao, S.G. Crane, A. Hime, W.A. Taylor, D. Tupa, D.J. Vieira, and H. Wollnik, *Phys. Rev. A* **58**, R1637 (1998).
  - [9] The relevant  $^{83}\text{Rb}$  trapping transitions were measured to be very close to those reported by Thibault *et al.* [10]. The  $^{84}\text{Rb}$   $5S_{1/2}$ ,  $F=3 \rightarrow 5P_{3/2}$ ,  $F'=4$  trapping transition was referenced directly to the  $5S_{1/2}$ ,  $F=3 \rightarrow 5P_{3/2}$ ,  $F'=2$  saturated absorption line in  $^{85}\text{Rb}$  and the  $^{84}\text{Rb}$   $5S_{1/2}$ ,  $F=2 \rightarrow 5P_{3/2}$ ,  $F'=3$  repump transition was generated from the second lower sideband produced by an EOM driven at 1.592 GHz.
  - [10] C. Thibault *et al.*, *Phys. Rev. C* **23**, 2720 (1981).
  - [11] T. Walker, D. Sesko, and C.E. Wieman, *Phys. Rev. Lett.* **64**, 408 (1990).
  - [12] S.D. Gensemer, V. Sanchez-Villicana, K.Y.N. Tan, T.T. Grove, and P.L. Gould, *Phys. Rev. A* **56**, 4055 (1997).
  - [13] W. Petrich, M.H. Anderson, J.R. Ensher, and E.A. Cornell, *Phys. Rev. Lett.* **74**, 3352 (1995).
  - [14] D.J. Vieira, S.J. Brice, S.G. Crane, A. Goldschmidt, R. Guckert, A. Hime, D. Tupa, and X. Zhao, in *Proceedings of the Trapped Charged Particles and Fundamental Physics Conference*, Asilomar, California, 1998, edited by D.H.E. Dubin and D. Schneider, AIP Conf. Proc. No. 457 (AIP, Woodbury, NY, 1998), p. 143.